Journal of
Tissue Science & Engineering

Poinern, J Tissue Sci Eng 2012, 3:3
DOI: 0.4172/2157-7552.1000119

Research Article Open Access

Biocompatibility of Synthesised Nano-Porous Anodic Aluminium Oxide Membranes for Use as a Cell Culture Substrate for Madin-Darby Canine Kidneys Cells: A Preliminary Study

GEJ Poinern[1]*, N Ali[1], C Berry[2], P Singh[3], S Berchmans[4] and D Fawcett[1]

[1]*Murdoch Applied Nanotechnology Research Group, Department of Physics, Energy Studies and Nanotechnology, School of Engineering and Energy, Murdoch University, Murdoch, Western Australia 6150, Australia*
[2]*School of Veterinarian and Biomedical Sciences, Division of Health Sciences, Murdoch University, Murdoch, Western Australia 6150, Australia*
[3]*School of Chemical and Mathematical Sciences, Murdoch University, Murdoch, Western Australia 6150, Australia*
[4]*Electrodics and Electrocatalysis Division, Central Electrochemical Research Institute (CECRI-CSIR), Karaikudi630006, Tamil Nadu, India*

Abstract

In this study we investigate for the first time the biomedical potential of using a membrane made from anodic aluminium oxide (AAO) for culturing the Madin-Darby Canine Kidney (MDCK) epithelial cell line. Nano-porous aluminium oxide membranes exhibit interesting properties such as high porosity, which allows the exchange of molecules and nutrients across the membrane and can be made with highly specific pore sizes that can be preselected by adjusting the controlling parameters of a temperature controlled two-step anodization process. The cellular response and interactions of the MDCK cell line with the synthesised nano-porous AAO membrane, a commercially available membrane and a glass control were assessed by investigating cell adhesion, morphology and proliferation. The number of viable cells proliferating over the surface of each respective membrane was quantified over a 72 h period and revealed that synthesised alumina membrane was at least comparable to the glass control substrate. Furthermore, both optical and electron microscopy investigations revealed distinct evidence of focal adhesion sites on the nano-porous membranes and the penetration of cellular extensions into the pore structure. The results of the study indicate that nano-porous AAO membranes have the potential to become practical cell culture substrates with the ability to enhance adhesion and proliferation of MDCK cells.

Keywords: Nano-porous anodic aluminium oxide; MDCK; Cell adhesion; Cell culture; Tissue scaffold

Introduction

Porous aluminium oxide membranes derived from the electrochemical process of anodization of aluminium metal has been studied in detail in a variety of polyprotic acids or electrolytes, temperatures and anodization voltages for more than sixty years [1]. Using the conventional anodization process in polyprotic acids (e.g., oxalic, phosphoric or sulphuric acid) a nano-porous oxide layer can be formed over the metal surface. Unfortunately, during the formation process, the resulting pores arrangement is quite disordered. However, in 1998, Masuda et al. [2] using a two-step anodization process was able to produce a highly ordered hexagonal pore structure from a set of pre-arranged macroscopic parameters. These controllable macroscopic parameters (acid type and concentration, temperature and applied voltage) dictated the resulting nanometer scale structure that is formed in the AAO layer, thus producing an array of pore diameters, periodicity and density distribution. Thus, the pore diameter is dependent on the electrolyte and applied voltage, while the thickness depends on the duration of the anodization process, which allows for the synthesis of porous structures with large aspect ratios [3,4]. These attractive features make AAO membranes an ideal template for a variety of nanotechnology applications that use them in the manufacture of nanometer scale materials and devices [5-7] or incorporate them into specific applications such as biological/chemical sensors [8,9], nano-electronic devices [10,11], filter membranes [12] and medical scaffolds for tissue engineering [13-15].

Cellular response and cell-substrate interactions are directly affected by the environment of the substrate on which the cells are cultured and can also have a profound influence on cell activity, adhesion, morphology and proliferation [16]. The sizes of cells are typically in the micrometre range, with their component structures and associated environment being in the sub-micrometre to nanometre range. The significance of the nanometre scale becomes apparent when you consider the molecular building blocks of life such as: proteins, carbohydrates, nucleic acids and lipids are all nanometre-sized structures. Therefore, cellular interactions with nanostructures such as proteins are crucial for controlling cell functions such as migration, proliferation, and the production of the extracellular matrix, (ECM) [17]. Furthermore, the physical structure and surface chemistry of the nanostructure can directly influence the behaviour of the cell when it comes in contact with the substrate surface. However, mechanisms behind the adhesive attachment of the cell, the influence of the surface in this interaction and how it subsequently influences the proliferation of anchorage-dependent cells is yet to be fully explained. For example, filopodial extensions from fibroblast cells are capable of sensing nanometre scale topographical features as small as 10 nm, even though they are many times larger than the surface feature itself [18]. It is due

***Corresponding author:** Dr. Gerrard Eddy Jai Poinern, Murdoch Applied Nanotechnology Research Group, Department of Physics, Energy Studies and Nanotechnology, School of Engineering and Energy, Murdoch University, Murdoch, Western Australia 6150, Australia, Tel: +61 8 9360-2892; Fax: +61 8 9360-6183; E-mail: g.poinern@murdoch.edu.au

Received August 02, 2012; **Accepted** September 12, 2012; **Published** September 17, 2012

Citation: Poinern GEJ, Ali N, Berry C, Singh P, Berchmans S, et al. (2012) Biocompatibility of Synthesised Nano-Porous Anodic Aluminium Oxide Membranes for Use as a Cell Culture Substrate for Madin-Darby Canine Kidneys Cells: A Preliminary Study. J Tissue Sci Eng 3:119. doi:10.4172/2157-7552.1000119

to this interplay between cell and nanometre scale topography that has generated so much interest in recent years. The interest stems from the potential ability of nanometre scale topographical surface features of a substrate being able to mimic components of the ECM and this solicits a favourable response from the cell to attach and proliferate [19]. It should also be mentioned that cells also respond to the layer of proteins that are normally deposited over the surface of a biocompatible substrate when it is immersed in a physiological fluid. During immersion, protein adsorption by the nanometre scale topographical surface features is highly dependent on the nature of the surface; for example surface charge, surface chemistry [20], wettability [21], surface density of cell-binding ligands [22] and nanometre scale topography [23] all play an important role in the cell-substrate interaction. It also highlights the importance of the nanometre scale topography in promoting protein adsorption, which ultimately decides the final performance of the substrate as an effective compatible biomaterial. For example, Yao et al. has recently shown that nanometre scale topographic enhancement of biocompatible implant materials promotes protein adsorption and the adhesion of osteoblast cells onto Ti_6Al_4V and anodized Ti surfaces [24,25]. While studies by Webster et al. [26] have revealed a significant enhancement in the ability of osteoblast cells when attaching to nano-ceramic materials.

The outcome of these studies clearly indicate that nanometre scale topographical features present on the surface of a biomaterial can have a significant influence on both protein adsorption and cell adhesion, which ultimately influences the performance of the biomaterial. In the case of nano-porous AAO membranes the dominant surface feature sensed by the cells, is the pore size of the membrane. The size sensing ability of osteoblast cells was confirmed by a study by Karlsson et al. [27]. This study found that by varying the pore size, it was indeed possible to control the secretion of specific protein species from the cell wall to the substrate, which in turn influenced cellular attachment, differentiation and mineralization taking place. In a similar study by Nguyen et al. [28] the cellular and molecular responses of smooth muscle cells to various nanometre size topographical features revealed their sensing capability and surface interaction.

Furthermore, the results of these studies suggest that it's the porous structure and topographical features of the AAO membrane that are influencing cellular behaviour. Therefore, the aim of the present study was to, for the first time, investigate the viability of using an engineered AAO membrane with fixed nanometre pore sized topographical features as a cell substrate for promoting cellular growth of MDCK cells for potential tissue engineering applications. The cells were cultured on two different kinds of nano-porous AAO membranes and a laboratory grade glass control. The first membrane was synthesised in-house, while the second was a commercially available membrane (Whatman® Anodisc 25, 0.1 μm). Both membranes had a mean pore diameter of 100 nm, but both had different inter-pore spacing and surface roughness. The cellular response of MDCK cells to both porous membranes and the glass control surface was evaluated over a 72 h period using the CellTiter 96® Aqueous One Solution cell proliferation assay procedure. Cell adhesion and morphology on all three substrates was investigated using optical microscopy and Field Emission Scanning Electron Microscopy (FESEM).

Materials and Methods

Materials

All chemicals used were of chemical grade purity, supplied from Sigma-Aldrich (Castle Hill, NSW, Australia) and used without further purification. CellTiter 96® Aqueous One Solution reagent was supplied by Promega, USA and was used to determine the number of viable cells proliferating over the surface of each respective substrate. Milli-Q® water (Barnstead Ultrapure Water System D11931; Thermo Scientific, Dubuque, IA) (18.3 MΩ cm^{-1}) was used throughout all synthesis procedures involving aqueous solutions.

Fabrication of nano-porous AAO membranes

The membrane fabrication process begins with a high purity (99.99%) 100 mm square Aluminium (Al) sheet, 0.25 mm thick supplied by Alfa Aesar, USA being cut up to form 50 mm x 20 mm strips. The individual strips are then annealed in nitrogen at 500°C for 5 hours to re-crystallise and release mechanical stresses in the strips. After annealing, the Al strips were degreased in acetone and then etched in 3.0 M sodium hydroxide for 5 minutes before being thoroughly washed in Milli-Q® water. The strips were then dried before a layer of polymer was applied onto one side of the strip. At this point, the strip was ready for the first step of the two-step anodization procedure. During the first step, the strip is anodized using a voltage of 60 V in an electrolyte solution of 0.3 M oxalic acid for 5 hours. At the end of the first anodization: the resulting thin layer of oxide formed on one side of the strip was removed from the substrate by immersion in a stirred acidic solution composed of phosphoric and chromic acid (70 mL/L and 20 g/L, respectively) at 60°C for 1 hour. This step was necessary to selectively remove the first oxide layer and expose a highly periodic and indented landscape covering the surface of the Al substrate. These indentations form the initiation sites for the subsequent formation of pores in the second anodization step [1,4,29]. The second anodization is performed under the same conditions as the first step, except the second step the anodization period is 3 hours. This gives rise to a regular, honeycomb arrangement of nanometre-sized pores that extend across the surface of the oxide layer. The nanometre sized pores are then widened by chemical etching in a 5% solution of phosphoric acid at 35°C for 15 minutes. Then a thin layer of Acrifix 192 was applied to the anodized side of the Al strip. This serves as a physical support for the membrane during the removal of the Al substrate using an acidic solution mixture composed of 0.1 M copper chloride and 7% hydrochloric acid. Following this; the barrier layer oxide was removed from the membrane by etching in phosphoric acid. The complete dissolution of the barrier layer and acrylic support results in providing a clear oxide membrane. The stage of processing involved the sterilization procedure, which consisted of immersing the membranes in a 30% solution of hydrogen peroxide at 60°C for 15 minutes. This was followed by quickly dipping the membrane into a solution of Milli-Q® water for 10 seconds to remove any hydrogen peroxide from the membrane surface and complete the sterilization procedure. The membranes were then allowed to dry before being stored in airtight containers ready for future characterization and cell studies applications. Figure 1 presents a field emission scanning electron microscopy micrograph of a representative in-house nano-porous AAO membrane fabricated using the two-step anodization procedure. The image highlights the high porosity, narrow pore size and inter-pore distance distribution of the in-house membrane used.

Cell culturing and growth on AAO membranes

Cell seeding and culture: The cells used in the *in vitro* study were the Madin-Darby Canine Kidney (MDCK) cell line and were supplied by the School of Veterinarian and Biomedical Sciences (Division of Health Sciences, Murdoch University, Murdoch, Western Australia 6150, Australia). The cells were originally stored, frozen in

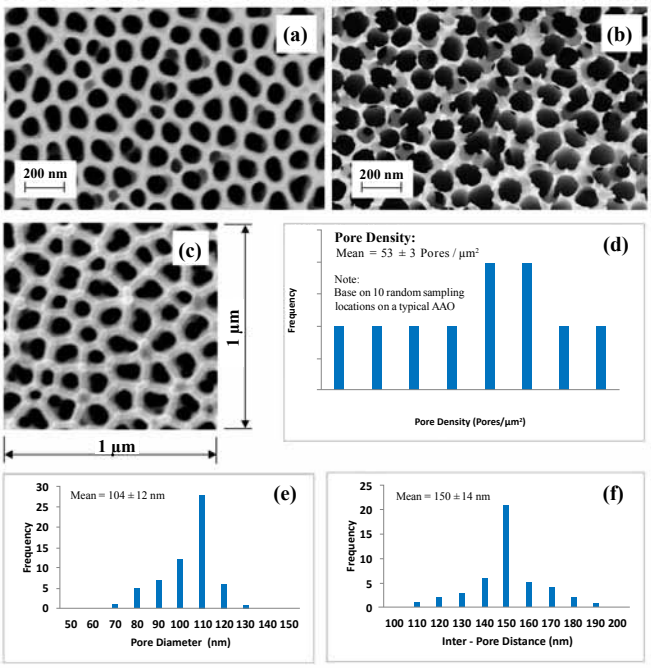

Figure 1: Characterization of in-house nano-porous membrane: a) in-house membrane; b) Whatman® anodisc membrane; c) typical 1 µm square analysis grid; d) histogram of mean pore density; e) histogram of mean pore diameter; and f) mean inter-pore distance.

liquid nitrogen and thus needed to be resuscitated. The resuscitation procedure consisted of rapidly thawing an aliquot of cells to room temperature and then adding the cells to a 5 mL medium solution pre-warmed to 37°C. The medium used was Dulbecco's Modified Eagle's Medium (DMEM) and contained 4500 mg of glucose/mL, 100 mg of sodium pyruvate, L-glutamine, penicillin streptomycin and 10% fetal calf serum (FCS) all supplied by Sigma Aldrich, Australia. The cell-medium solution was then centrifuged at 200 g for 10 minutes, after which the supernatant was discarded and the cells were re-suspended in a medium of DMEM and 10% FCS. Then a 1 mL sample of the cell-medium solution was added to 75 cm^2 tissue culture flasks, each containing 10 mL of a medium containing DMEM and 10% FCS. The cells were then incubated at 37°C with a 5% CO_2 atmosphere until a confluent layer of cells formed on the bottom of the flask. At this point sub-culturing of cells was started. During this procedure, the medium was removed from each flask and the remaining cells were washed twice, each time with a fresh 10 mL phosphate buffer solution (PBS). Then a 2 mL solution composed of two active ingredients, namely trypsin and ethylenediaminetetraacetic acid (EDTA) (0.05% trypsin and 0.01% EDTA, with the balance of the solution made up by double distilled water) were added to each flask. Each flask was then gently agitated until the solution was evenly spread over its bottom before the cells were incubated at 37°C for a further 20 minutes. At the end of this time, the cells in each flask were dislodged from the flask bottom by agitation. Then a 10 mL solution of DMEM, containing a 10% solution of FCS was added to each flask to aid in the neutralization of trypsin. The cells were then collected and transferred into a clean tube before being centrifuged at 1000 rpm for 5 minutes at 40°C. At the end of centrifuging the solution, the supernatant was removed and the cells were re-suspended in a 3 mL solution of DMEM culture medium containing 10% FCS. After suspension, a 1 mL aliquot of cells and medium was transferred into a new flask containing a 10 mL solution of DMEM. The cells were then incubated at 37°C with a 5% CO_2 atmosphere until confluence in conventional tissue culture flasks.

Cell adhesion studies: Both the in-house synthesised nano-porous AAO membrane and the commercially available Whatmann® Anodisc were used without any further surface treatment. Before cell seeding the membranes and glass controls underwent the sterilization procedure as discussed earlier. The procedure consisted of 4 samples of each nano-membrane type and glass control, with 1 sample set being used for each time interval. The time intervals consisted of 4, 24, 48 and 72 h. A total of 12 membranes and glass controls were individually placed into a well of a 24 well cell culture plate supplied by Cellstar® Greiner Bio-One, Germany. Then 1 mL of solution of MDCK cells (1 x 10^5 cells/mL) suspended in DMEM culture medium and 10% FCS were transferred to each well of the culture plate using a pipette. Then a further 1 mL of DMEM medium was added to each well using a pipette. The cells were then incubated at 37°C with a 5% CO_2 atmosphere for 4 h. After 4 h, the first 3 membranes, located in the 4 h row of the culture plate were removed from their wells and washed several times using a PBS to remove unattached cells and DMEM medium. The remaining 9 membranes were then transferred from their wells and placed into wells with fresh culture medium on another 24 well cell culture plate. The transfer procedure ensured that unattached cells were removed and the original depleted culture medium was replenished. The cells were then incubated at 37°C with a 5% CO_2 atmosphere for a further 24 h. After being cleaned the first 3 membranes, were then prepared for microscopy and cell adhesion studies. After 24 h, a similar procedure to that discussed above was followed. The next 3 membranes, from the 24 h line on the culture plate were removed and prepared for microscopy while the remaining 6 membranes were then transferred to a new plate with fresh culture medium in the wells and the method was again repeated for both the 48 and 72 h time periods. Furthermore, the cell adhesion procedure was carried out in triplicate to ensure consistency in the study.

Cell proliferation assay: The number of viable MDCK cells proliferating over the surface of each respective membranes and glass controls were quantified over a 72 h period using the CellTiter 96® Aqueous One Solution cell proliferation assay procedure. The cell proliferation procedure consisted of preparing a 24 well cell culture plate supplied by Cellstar® Greiner Bio-One, Germany to contain a set of membranes and glass controls. Three culture plates were used in total during the procedure, thus making up a triplicate set of results. A set of 4 samples of each membrane type and glass control were individually placed into a separate well of a cell culture plate, with each sample set being used for each time interval (4, 24, 48 and 72 h). The wells were then filled by adding a 1 mL solution of MDCK cells (1 x 10^5 cells/mL) suspended in DMEM culture medium with 10% FCS and 1% PBS using a pipette. The cells were then incubated at 37°C in a humidified, 5% CO_2 atmosphere for 4 hours. After 4 hours, the first 3 samples were then transferred to wells, pre-filled with 500 µL of fresh culture medium, located on a new cell culture plate. The evaluation of the initial cell proliferation was carried out by adding a 60 µL solution of CellTiter 96® Aqueous One Solution reagent to the wells using a pipette and then following the suppliers procedures. The cells were then incubated at 37°C in a humidified, 5% CO_2 atmosphere for a further 1 h. Meanwhile, the remaining 24, 48 and 72 h samples on the original culture plate were then transferred to a new culture plate, with wells prefilled with 500 µL of fresh culture medium. These cells were then incubated at 37°C in a humidified, 5% CO_2 atmosphere for a further proliferation period. After the additional 1 h, the 4 h samples were removed from

the incubator and 3 aliquot of 120 µL were removed from each of the 3 wells. Then each individual aliquot was placed into a fresh well located on a 96 Well Tissue Culture Plate (83.1835, Sarstedt Inc. Newton, USA). Then the absorbance at 490 nm was recorded using an ELISA 96 well automatic plate reader fitted with a Microplate Spectrophotometer equipped with Microplate Manager 5.2.1 software for data analysis (Bio-Rad, Australia). The procedure was then repeated for the 24, 48 and 72 h proliferation periods.

Statistical analysis

Major surface features such as pore density, pore diameter and inter-pore distance are presented as mean ± standard deviation. The frequency and size of the particular surface features were determined by counting and physically measuring the size of the features found within 10 randomly selected 1 µm square grids. The results of this analysis are presented in Figure 1. The cell proliferation data obtained from the CellTiter 96® Aqueous One Solution cell proliferation assay (n = 36 membranes, including triplicates) were analysed using Microplate Manager 5.2.1 software for data analysis (Bio-Rad, Australia). The mean ± standard deviation of the cell proliferation study is presented in Figure 2(e).

Characterization of Materials

The fabricated nano-porous AAO membranes and Whatmann® Anodisc membranes were examined by field emission scanning electron microscopy (FESEM). The micrographs were taken using a Zeiss Neon EsB FIBSEM. The field emission electron gun provided both high brightness and high resolution (0.8 nm). Samples were mounted on individual substrate holders using carbon adhesive tape before being sputter coated with a 2 nm layer of platinum to prevent charge build up. Micrographs were taken at various magnifications ranging from 2 to 5 kV using the SE2 and InLens detectors.

Optical microscopy was used throughout the cell studies to examine cell-membrane interactions such as attachment and proliferation. An Olympus BX51 compound microscope (Olympus Optical Co. Ltd., Tokyo, Japan) was used for all optical studies and photographs were taken using the DP 70 camera attachment. Before microscopy observation, the adhering cells on each membrane were fixed by immersing the respective membrane in a 500 µL solution of 2.5% glutaraldehyde at 4°C overnight. The following day, washing the membranes several times with PBS removed the glutaraldehyde. The cells were then stained using an aqueous solution containing 1% Fuchsin acid. After 30 minutes the excess stain was rinsed off the membranes using double distilled water. After the membranes had dried they were then ready for optical microscopy investigation. Before FESEM observation, the membranes were washed in a 30% solution of ethanol several times before being allowed to soak for 15 minutes in the ethanol solution. At the end of this period, sequential drying of the samples using progressively increasing concentrations of ethanol washes (2 washers of 50%, 70%, 80%, 90%, and 95%), until being finally washed in 100% ethanol for 30 minutes. Following the ethanol washing procedure, the samples were then treated with a 50:50 solution of ethanol: amylacetate for 30 minutes. This was then followed by 2 immersions in amylacetate over a period of 1 h before being placed into a critical point dryer. Finally, the dried samples were mounted on FESEM stubs before being sputter-coated with a 2 nm layer of platinum metal for imaging purposes. The samples were then ready for FESEM investigations.

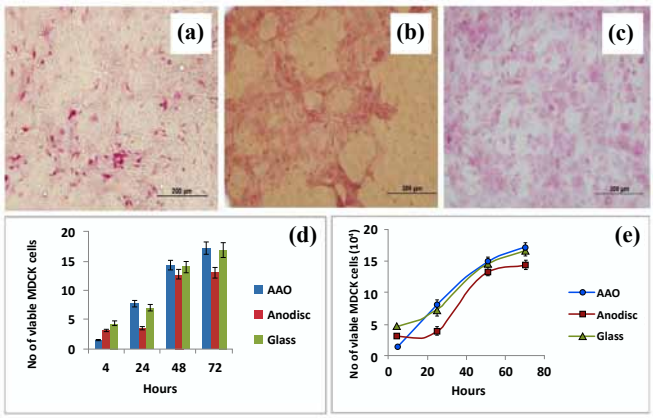

Figure 2: Optical microscopy of cells proliferation at the 24 h period; a) in-house AAO membrane; b) Whatman® anodisc membrane; c) glass substrate control; d) a typical 72 h cell proliferation assay; and e) comparison between the number of viable cells on an in-house AAO membrane, Whatman® anodisc membrane and a glass control. Scale bars in (a), (b) and (c) are 200 µm.

Results and Discussions

The unique structure and surface topography of synthesised nano-porous AAO membranes were investigated using field emission scanning electron microscopy (FESEM). The refined two-step anodization process is straightforward, economical and permits the selection of material properties such as membrane thickness, pore size, inter-pore spacing and pore density in a reproducible manner. The high open porosity of the nano-porous membrane has the potential to be a beneficial substrate for culturing a variety of different cell types, such as MDCK. However, to date, no work has been done to investigate cellular responses of the MDCK cell line to nano-porous AAO membranes or the viability of using the membrane as cell substrate for this epithelial cell line. The present study focused on the nanometre scale surface topographical features of the in-house manufactured nano-porous AAO membrane and a commercially available alumina membrane (Whatmann® Anodisc) compared to a glass control. The study also examined cell attachment and a cell proliferation assay was performed over a 72 h period to determine the viability of using the nano-porous AAO membrane as a cell substrate.

The material's surface investigation was conducted using FESEM, which was used to study nanometre scale surface topographical features of both the in-house and commercial nano-porous membranes. The surface terrain of the in-house nano-porous AAO membranes revealed an architecture that was highly ordered, with close packed hexagonal arrays of uniformly sized pores. The ordered pore domains are tessellated across a smooth undulating surface landscape as shown in Figure 1(a). Examination of the FESEM micrographs, reveal the presence of occasional non-ordered pores between the pore domains. The non-ordered pores, which have also been reported by other researchers, result from inevitable point defects, dislocations and grain boundaries in the original Al substrate [30,31]. Also present in the micrographs are a small number of minor pores merging with larger, nearby neighbouring pores to form elliptical shaped pores. Analysis of several 1 µm^2 survey locations (Figure 1(c)) that were randomly selected from various locations across the membrane, revealed a pore density of 53 ± 3 pores/µm^2 (mean ± std), see Figure 1(d). Subsequent analysis of the sample determined a mean pore diameter of 104 ± 12 nm and a mean inter-pore distance of 150 ± 14 nm, see Figures 1(e) and (f). Inspection of the pore density histogram in Figure 1(d) reveals a small variation in pore densities found across the membrane, a similar

narrow size distributions can be seen for both the pore diameter and inter-pore distance histograms in Figures 1(e) and (f) respectively. The narrow size distribution in these nanometre scale features is a clear demonstration of the two-step anodization techniques ability to consistently produce a highly regular, closely packed and uniform array of pores. This consistency was extremely important since the subsequent *in vitro* cell studies needed to be carried out on membrane surfaces with a regular surface topography.

The other nano-porous membrane used throughout the research work for comparative purposes, (since it had a similar pore size) was the commercially available Whatman® Anopore (Anodisc) membrane [32]. The Anodisc inorganic membrane is composed of a high purity alumina matrix, with a honeycomb pore structure. The pores are circular in shape, have little variation in size and are available in 3 nominal pore sizes: 0.02 μm, 0.1 μm and 0.2 μm, with a nominal thickness of 60 μm. The Anodisc membranes have a porous structure that creates nano-channels that traverses the entire depth of the membrane, with no lateral crossovers between individual channels. This structure makes these membranes well suited for a wide range of laboratory filtration applications [32]. The manufacturer's specification contains no information regarding the type of synthesis process used to produce their membranes or details of size variation of pore diameter and inter-pore distance. Analysis of the pore geometry and diameter using the same measuring techniques used for the in-house manufactured AAO membranes revealed that the Anodisc's mean pore diameter is 120 ± 45 nm. The mean distance between pores, calculated from the nominal density of pores is estimated to be around 0.32 μm, however, X-ray diffraction studies of Anodisc filters by Fisch et al. [33] found a mean distance of around 0.37 μm. Their results also revealed that there was very little difference in the X-ray spectra from 0.1 and 0.2 μm pore sizes and subsequent simulations of model spectra confirmed the mean inter pore distance of 0.37 μm. Inter-pore distance measurements reveal that the mean pore distance is between 0.32 μm to 0.37 μm on the anodisc samples used in this work. However, it should be pointed that despite having a fairly consistent pore geometry and distribution, with no apparent pore domains present, the anodisc membranes have the largest variation in pore geometry and inter-pore spacing. In addition, the pore wall thickness is not consistent across the membrane, with many very rough edges that protrude up from the surface along many of these inter-pore walls, see Figure 1(b). Overall, the landscape of the anodisc membrane is very rough compared to the in-house fabricated membranes which are smooth and undulating, with a more refined nano-topography.

Optical microscopy investigations of MDCK cells after 24 h of cultivation on all three substrates reveal good cell adhesion; with a flattened polygonal morphology and wide spread coverage over the substrate surfaces, see Figure 2. Examination of Figure 2(a), Figure 2(b) and Figure 2(c) reveal that the cells cultured on the nano-porous membranes are comparable to those cultured on the glass control substrate. Furthermore, the surface of the cells was covered by numerous microvilli which extended from the cells to a length of several micrometres. Besides increasing the surface area of the cell, the microvilli are actively involved in adsorption, cellular adhesion and secretion [34], their presence clearly indicates that the cells are interacting with the ECM and the nano-porous membranes, see Figure 3(c), Figure 3(d) and Figure 3(e). The FESEM micrographs generated also reveal the presence of filopodia at the cell boundaries, which spread out over the surface of the nano-porous membranes using the pores as anchorage points. There is also indications that long thin filopodia (< 100 nm in diameter) are also penetrating into the upper region of the pore structure to enhance their attachment to the nano-porous surface, see Figure 3(f).

Even though the glass substrate didn't have the nanometre scale topographical features of the two membrane types, the cells still attached and were homogeneously distributed over the entire surface of the substrate. Examination of the optical microscopy images presented in Figure 2(a), Figure 2(b) and Figure 2(c) for 24 hours of cultivation revealed that the bulk of the surfaces on all three membranes were covered with cells. The results of the adhesion studies clearly demonstrated cell attachment and interaction on both nano-porous membranes and the glass control, but did not provide any biological information regarding the long-term viability of cell survivability. Therefore, a cell proliferation assay was carried out since proliferation is an important factor in determining the long-term survival of cells on a tissue culture substrate or tissue engineering scaffold potential. Figure 2(b) presents the results of the cell proliferation assay carried out over a 72 h period. During the assay there was no evidence of infection or toxicity effects occurring to the cells over the test period.

After the first 4 h, the number cells adhering to the glass control was higher than both of the nano-porous membranes. Significantly more cells were present on the Whatman® Anodisc membrane (71.2% compared to the glass control) than those on the in-house AAO membrane (33.3% compared to the glass control). During the following days, the number of viable cell proliferating on all substrates continued to increase. By the end of the 24 h period the number of viable cells on the in-house nano-porous AAO membrane was 9.8% greater than the glass control and significantly greater than the Whatman® anodisc membrane, (which was only 52% of the cell growth on the glass control). From this point on, the Whatman® anodisc membrane was always significantly less than both the in-house AAO membrane and

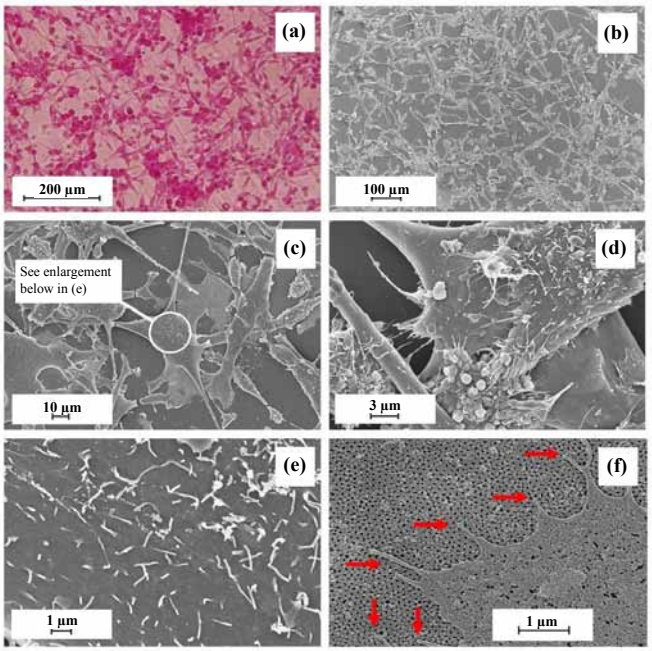

Figure 3: a) Optical microscopy of MDCK cells on in-house AAO membrane; b) FESEM image of cells on in-house AAO membrane; c) and d) detailed image of cells on AAO membrane; e) enlargement of cell membrane showing microvilli; and f) enlargement of cell membrane showing the presence of filopodia (red arrows). Scale bars shown on each image.

glass control. At the 48 h period, the in-house AAO membrane was 2.2% greater than the glass control and greater than the Whatman® anodisc membrane which was 90.8% the value of the glass control. And by the 72 h time period, both the in-house AAO membrane and the glass control are comparable with the AAO membrane having 1.8% more viable cells than the glass control. At the end of the 3 day proliferation assay the highest number of viable cells were found on the in-house AAO membrane, while the lowest number of viable cells was found on Whatman® anodisc membrane.

A direct comparison between the in-house AAO membrane and the glass control is presented in Figure 2(e). Initially, the glass control has the largest number of viable cells attached to its surface, but by the 20 h period, cell proliferation on in-house AAO membrane is comparable with the glass control. From the 20 h period, the number of viable cell numbers on the in-house AAO membrane is marginally greater than that of the glass control. During the 72 h period; the overall proliferation rate was found to be slower for cells cultured on the Whatman® anodisc membranes, this is despite of the initial superior number of viable cells recorded at the 4 h period. From the 4 h period onwards, the number of viable cell numbers on the Whatman® anodisc membranes is consistently less than both the in-house membranes and glass controls. One possible factor that maybe influencing cell behaviour and proliferation on the Whatman® anodisc membranes is the many very rough edges that protrude up from the surface along the pore walls. The roughness caused by these protrusions tends to nano-texture the surface of the membrane, which is significantly different from both the in-house AAO membranes and the glass controls. At the end of the 72 h cell proliferation assay the number of viable MDCK cells on the in-house AAO membrane was 17.3 x 10^4, while the number of cells on the glass control was 17.0 x 10^4. The study indicates that the in-house AAO membrane was capable of being used successfully as a cell culture substrate for the MDCK cell line. The assay also suggests that the increased surface roughness of the Whatman® anodisc membranes had influenced the MDCK cell behaviour which resulted in lower numbers of viable cells attaching and by the 48 h period the number of viable cells on the membrane had levelled out, see Figure 2(d). This suggests that it may be possible to influence MDCK cell behaviour and proliferation by nano-texturing the surface of a membrane in a similar nanometre scale surface topography to the Whatman® anodisc membranes.

The importance of this study in progressing potential tissue engineering applications using AAO membranes as a cell substrate is derived from the current biomedical use of the MDCK cell line as a general model for epithelial cells. Epithelia cells are tightly packed and organized into sheets that form epithelium tissue, which is mainly found covering the internal organs and other surfaces linings within the body. To treat damaged surface and lining epithelia, cells and biocompatible substrates such as AAO membranes upon which cells can attach and proliferate rapidly are the key components of this technology. This study confirms that it is possible to culture MDCK epithelial cells that retain histological characteristics and proliferation rates that can be used to produce a confluent layer over the AAO membrane. Future studies will be needed to examine the further potential of lifting the cellular layer from the membrane and directly applying it to prepared receiving wound bed were it is expected to enhance the treatment of damaged surface and lining epithelia.

Conclusion

The present preliminary study has established that an in-house nano-porous AAO membrane has the biomedical potential for culturing the Madin-Darby Canine Kidney (MDCK) cell line. The membrane material was used without any further surface modification and showed no cytotoxic effects during the 72 h cell proliferation assay. Cells were seen to adhere to both membrane types, with the presence of thin filopodia clearly anchoring the cells to the nano-porous surface. The number of viable cells at the end of the 72 h cell proliferation assay revealed that the in-house nano-porous membrane was comparable to the glass control.

Acknowledgements

This work was partly supported by the Western Australian Nanochemistry Research Institute (WANRI). Dr. Derek Fawcett would like to thank the Bill & Melinda Gates Foundation for their research fellowship. The authors would like to thank Ms Catherine Rinadli and Ms Ianthe Pitout for their assistance with the cell study.

Disclosure

The authors report no conflict of interest in this work.

References

1. Poinern GEJ, Ali N, Fawcett D (2011) Progress in Nano-Engineered Anodic Aluminium Oxide Membrane Development. Materials 4: 487-526.
2. Masuda H, Yada K, Osaka A (1998) Self-ordering of cell configuration of anodic porous alumina with large-size pores in phosphoric acid solution. Jpn J Appl Phys 37: L1340-L1342.
3. O'Sullivan JP, Wood GC (1970) The morphology and mechanism of formation of porous anodic films on aluminium. Proc R Soc London 317: 511-543.
4. Li AP, Muller F, Birner A, Nielsch K, Gosele U (1998) Hexagonal pore arrays with a 50-420 nm interpore distance formed by self-organization in anodic alumina. J Appl Phys 84: 6023-6026.
5. Shingubara S (2003) Fabrication of nanomaterials using porous alumina templates. J Nanopart Res 5: 17-30.
6. Han N, Deng P, Chen J, Chai L, Gao H, et al. (2010) Electrophoretic deposition of metal oxide films aimed for gas sensors application: the role of anodic aluminum oxide (AAO)/Al composite structure. Sens Actuators B Chem 144: 267-273.
7. Chen J, Xu L, Li W, Gou X (2005) α-Fe2O3 Nanotubes in gas sensor and lithium-ion battery applications. Adv Mater 17: 582-589.
8. Kim Y, Jung B, Lee H, Kim H, Lee K, et al. (2009) Capacitive humidity sensor design based on anodic aluminum oxide. Sens Actuators B Chem 141: 441-446.
9. Poinern GE, Fawcett D, Ng YJ, Ali N, Brundavanam RK, et al. (2010) Nanoengineering a biocompatible inorganic scaffold for skin wound healing. J Biomed Nanotechnol 6: 497-510.
10. Kim JR, Oh H, So HM, Kim JJ, Kim J, et al. (2002) Schottky diodes based on a single GaN nanowire. Nanotechnology 13: 701-709.
11. Huang Y, Duan X, Cui Y, Lauhon LJ, Kim KH, et al. (2001) Logic gates and computation from assembled nanowire building blocks. Science 294: 1313-1317.
12. Jirage KB, Hulteen JC, Martin CR (1997) Nanotubule-based molecular-filtration membranes. Science 278: 655-658.
13. Karlson M (2004) Nano-porous aluminia, a potential bone implant coating. Acta Universitatis Upsaliensis. Comprehensive Summaries of Uppsala Dissertations from the Faculty of Science and Technology 997: 1-75.
14. Wu ZJ, He LP, Chen ZZ (2006) Fabrication and characterization of hydroxyapatite/ Al_2O_3 biocomposite coating on titanium. Trans Nonferrous Met Soc China 16: 259-266.
15. Poinern GEJ, Shackleton R, Mamun SI, Fawcett D (2010) Significance of novel bioinorganic anodic aluminium oxide nanoscaffolds for promoting cellular response. Nanotechnol Sci Appl 2011: 11-24.
16. Roach P, Eglin D, Rohde K, Perry CC (2007) Modern biomaterials: a review - bulk properties and implications of surface modifications. J Mater Sci Mater Med 18: 1263-1277.

17. Yim EK, Leong KW (2005) Significance of synthetic nanostructures in dictating cellular response. Nanomedicine 1: 10-21.

18. Dalby MJ, Riehle MO, Johnstone H, Affrossman S, Curtis AS (2004) Investigating the limits of filopodial sensing: a brief report using SEM to image the interaction between 10 nm high nano-topography and fibroblast filopodia. Cell Biol Int 28: 229-236.

19. Anselme K, Davidson P, Popa AM, Giazzon M, Liley M, et al. (2010) The interaction of cells and bacteria with surfaces structured at the nanometre scale. Acta Biomater 6: 3824-3846.

20. Rappaport C (1972) Small aspect of the growth of mammalian cells on glass surfaces. The chemistry of bio surfaces, Marcel Dekker 449-489.

21. Volger EA (1993) Interfacial chemistry in biomaterials science. In Berg J Wettability Marcel Dekker NY 184-250.

22. Grinell F (1978) Cellular Adhesives and extracellular substrata. Int Rev Cytology Academic Press NY 67-145.

23. Christenson EM, Anseth KS, van den Beucken JJ, Chan CK, Ercan B, et al. (2007) Nanobiomaterial applications in orthopedics. J Orthop Res 25: 11-22.

24. Webster TJ, Smith TA (2005) Increased osteoblast function on PLGA composites containing nanophase titania. J Biomed Mater Res A 74: 677-686.

25. Yao C, Slamovich EB, Webster TJ (2008) Enhanced osteoblast functions on anodized titanium with nanotube-like structures. J Biomed Mater Res A 85: 157-166.

26. Webster TJ, Ergun C, Doremus RH, Siegel RW, Bizios R (2000) Enhanced functions of osteoblasts on nanophase ceramics. Biomaterials 21: 1803-1810.

27. Karlsson M, Pålsgård E, Wilshaw PR, Di Silvio L (2003) Initial in vitro interaction of osteoblasts with nano-porous alumina. Biomaterials 24: 3039-3046.

28. Nguyen KT, Shukla KP, Moctezuma M, Tang L (2007) Cellular and molecular responses of smooth muscle cells to surface nanotopography. J Nanosci Nanotechnol 7: 2823-2832.

29. Ghorbani M, Nasirpouri F, Irajizad A, Saedi A (2006) On the growth sequence of highly ordered nanoporous anodic aluminium oxide. Mat Design 27: 983-988.

30. Napolskii KS, Roslyakov IV, Eliseev AA, Byelov DV, Petukhov AV, et al. (2011) The kinetics and mechanism of long-range pore ordering in anodic films on aluminium. J Phys Chem C 115: 23726-23731.

31. Yu WH, Fei GT, Chen XM, Xue FH, Xu XJ (2006) Influence of defects on the ordering degree of nanopores made from anodic aluminium oxide. Phys Lett A 350: 392-395.

32. Whatman® Anopore www.whatman.com/products

33. Fisch MR, Primak A, Kumar S (2002) X-ray diffraction study of Anodisc filters. Phys Rev E Stat Nonlin Soft Matter Phys 65: 046615.

34. Schäfer C, Borm B, Born S, Möhl C, Eibl EM, et al. (2009) One step ahead: role of filopodia in adhesion formation during cell migration of keratinocytes. Exp Cell Res 315: 1212-1224.